

A quadrature based method of moments for nonlinear Fokker–Planck equations

This article has been downloaded from IOPscience. Please scroll down to see the full text article.

J. Stat. Mech. (2011) P09031

(<http://iopscience.iop.org/1742-5468/2011/09/P09031>)

View [the table of contents for this issue](#), or go to the [journal homepage](#) for more

Download details:

IP Address: 130.192.35.110

The article was downloaded on 29/03/2012 at 17:48

Please note that [terms and conditions apply](#).

A quadrature based method of moments for nonlinear Fokker–Planck equations

Dustin L Otten and Prakash Vedula

School of Aerospace and Mechanical Engineering, University of Oklahoma,
Norman, OK 73019-0601, USA

E-mail: dustin.otten@lmco.com and pvedula@ou.edu

Received 4 October 2010

Accepted 5 September 2011

Published 30 September 2011

Online at stacks.iop.org/JSTAT/2011/P09031

[doi:10.1088/1742-5468/2011/09/P09031](https://doi.org/10.1088/1742-5468/2011/09/P09031)

Abstract. Fokker–Planck equations which are nonlinear with respect to their probability densities and occur in many nonequilibrium systems relevant to mean field interaction models, plasmas, fermions and bosons can be challenging to solve numerically. To address some underlying challenges, we propose the application of the direct quadrature based method of moments (DQMOM) for efficient and accurate determination of transient (and stationary) solutions of nonlinear Fokker–Planck equations (NLFPEs). In DQMOM, probability density (or other distribution) functions are represented using a finite collection of Dirac delta functions, characterized by quadrature weights and locations (or abscissas) that are determined based on constraints due to evolution of generalized moments. Three particular examples of nonlinear Fokker–Planck equations considered in this paper include descriptions of: (i) the Shimizu–Yamada model, (ii) the Desai–Zwanzig model (both of which have been developed as models of muscular contraction) and (iii) fermions and bosons. Results based on DQMOM, for the transient and stationary solutions of the nonlinear Fokker–Planck equations, have been found to be in good agreement with other available analytical and numerical approaches. It is also shown that approximate reconstruction of the underlying probability density function from moments obtained from DQMOM can be satisfactorily achieved using a maximum entropy method.

Keywords: large deviations in non-equilibrium systems, diffusion

Contents

1. Introduction	2
2. DQMOM formulation for a general nonlinear FPE	4
3. Linear Fokker–Planck equation in one dimension	6
4. Nonlinear Fokker–Planck equations	9
4.1. The Shimizu–Yamada model	9
4.2. The Desai–Zwanzig model	10
4.3. Fermions and bosons	15
5. Conclusion	16
Appendix. Derivation of the Fokker–Planck equation governing fermions and bosons	18
References	19

1. Introduction

The solution and characterization of stochastic systems is of great interest to engineers and scientists in many fields [1, 2]. Such systems often involve Fokker–Planck equations of (i) linear or (ii) nonlinear kind, that describe the evolution of the underlying probability density functions. The former kind of Fokker–Planck equations which are linear equations with respect to the probability density functions (even though the microscopic or Langevin dynamics is nonlinear) arise in stochastic systems exhibiting diffusion (or Markovian) processes. In contrast, nonlinear Fokker–Planck equations (NLFPEs), which involve nonlinearities with respect to the probability density functions, can be used to describe complex system behavior involving anomalous diffusion, quantum distributions, stochastic feedback and mean field interactions. Some applications of NLFPEs include plasma physics [3]–[5], classical models of fermions and bosons [6]–[14], surface physics [15, 16], nonlinear hydrodynamics [17]–[19], and neurosciences [20]–[22].

The linear Fokker–Planck equation (FPE) describing the Ornstein–Uhlenbeck (OU) process is one of the few FPEs that has exact analytic stationary and transient solutions [1, 2]. The Shimizu–Yamada (SY) model was phenomenologically derived for muscular contractions [23], and was later modified to describe a nonlinear stochastic mean field by Kometani and Shimizu [24]. So, unlike the OU process, the SY model is a nonlinear FPE with respect to its probability density. The analytic solutions for the transient mean and variance have been shown in the text by Frank [2]. Kometani and Shimizu [24] further modified their model to describe the controlling and regulating of interaction between a macroscopic supersystem and its weakly coupled microscopic subsystem [25, 26]. Desai and Zwanzig [25] analyzed this model and derived a nonlinear Fokker–Planck equation which can be described as a self-consistent dynamic mean field FPE [26]. Although no transient analytical solutions have been found for this equation, a broad range of numerical methods [27, 26, 25, 28] have been used to study the Desai–Zwanzig model. Nonlinear

Fokker–Planck equations have also been derived for the quantum mechanical topic of classical models of fermions and bosons [6]–[8], [10]–[14]. These equations do have well known stationary solutions, but the transient solutions have not been well studied.

Considering the broad range of applications of Fokker–Planck equations, a method to efficiently solve them is desired. Unfortunately, there exist very few Fokker–Planck equations which can be solved analytically. Due to this, many numerical models and methods have been proposed and used to analyze linear and nonlinear Fokker–Planck equations [27], including Monte Carlo techniques [29], cumulant moment expansion methods [25, 30], path-integral techniques [31, 5, 32], eigenfunction expansions [33, 34] and finite-difference methods [35]–[37], [13]. It was shown that the use of finite-difference methods for nonlinear Fokker–Planck equations could lead to stiff systems of ordinary differential equations [26]. Drozdov and Morillo [27] proposed an implicit finite-difference method based on a K -point Stirling interpolation formula. This method allowed for an increase in accuracy without much increase in the number of grid points. They successfully applied this to the relaxation dynamics for the nonlinear self-consistent dynamic mean field Fokker–Planck equation describing muscular contraction [24]. They also applied it with limited success to the more complete statistical-mechanical model given by Desai and Zwanzig [25]. Following the work of Drozdov and Morillo, Zhang *et al* [26] utilized a distributed approximating functional (DAF) [38, 39] based method for the solution of the so called Desai–Zwanzig model [25]. This method takes advantage of the integral relations of the Dirac delta function and its derivatives. These relations and their derivatives are then approximated by a Hermite polynomial whose integrals are discretized on a grid [26]. The goal of Zhang *et al* was to analyze the validity of a long-lived transient bimodality captured by Drozdov and Morillo [26, 27] and explain its occurrence.

The direct quadrature method of moments (DQMOM), first developed by Fox *et al* [40]–[42] in the context of population balance equations, is presented in this paper as an accurate and efficient alternative to other computational methods for the solution of nonlinear Fokker–Planck equations. DQMOM has many advantages over other methods and has recently been studied for obtaining solutions to the Boltzmann equation [43], for one-dimensional and two-dimensional noisy van der Pol oscillators [44], for linear Fokker–Planck equations describing aeroelasticity [45], for polydisperse gas–solid flows [46, 47] and for nonlinear filtering and control [48]. DQMOM approximates a density function as a collection of discrete Dirac delta functions which have associated weights and abscissas. Using constraints on the moments of the equation, one can obtain evolution equations for solving the unknown weights and abscissas. These weights and abscissas are then used to compute low order moments. In the current work, DQMOM will be used to compute numerical solutions to nonlinear Fokker–Planck equations for the first time (most previous works on DQMOM were for linear Fokker–Planck equations). Comparisons of stationary and transient solutions obtained from DQMOM will be made with those obtained from other analytical and/or numerical solutions. While DQMOM enables direct evaluation of moments, it will also be shown that these low order moments are sufficiently accurate to allow for satisfactory reconstruction of the underlying probability density functions using a maximum entropy method.

The rest of this paper is organized as follows. The formulation of DQMOM for solution of a general nonlinear Fokker–Planck equation is presented in section 2. In section 3 we will evaluate the accuracy of DQMOM by comparing the numerical solutions obtained

from DQMOM with corresponding analytical solutions for a linear FPE characterizing the Ornstein–Uhlenbeck process. After demonstrating the accuracy of DQMOM for a simple linear case, section 4 will demonstrate the accuracy of DQMOM for three representative nonlinear Fokker–Planck equations describing (i) the Shimizu–Yamada model, (ii) the Desai–Zwanzig model (relevant to muscular contraction) and (iii) fermions and bosons. This work concludes with a brief summary of the results and a glance at future work in section 5.

2. DQMOM formulation for a general nonlinear FPE

Given the general univariate Langevin equation

$$\frac{dX(t)}{dt} = -D(X, t, f) + \sqrt{Q(X, t, f)}\Gamma(t), \quad (1)$$

where Γ is the Langevin force, $D(X, t, f)$ is the drift coefficient, $Q(X, t, f)$ is the diffusion coefficient and $f \equiv f(x, t)$ denotes the underlying probability density function (PDF), the Langevin force has the following correlations:

$$\langle \Gamma(t) \rangle = 0, \quad \langle \Gamma(t)\Gamma(t') \rangle = 2\delta(t - t'). \quad (2)$$

The nonlinear Fokker–Planck equation in terms of the probability density function (PDF), $f(x, t)$, that is equivalent to the above Langevin equation can be expressed as

$$\frac{\partial f(x, t)}{\partial t} = -\frac{\partial}{\partial x}[D(x, t, f)f(x, t)] + \frac{\partial^2}{\partial x^2}(Q(x, t, f)f(x, t)). \quad (3)$$

Note that in general nonlinear Fokker–Planck equations, the drift and diffusion coefficients can depend on the underlying probability density functions.

In the DQMOM approximation, the PDF is approximated as a weighted summation of Dirac delta functions [42]:

$$f(x, t) = \sum_{i=1}^M w_i(t)\delta(x - x_i(t)), \quad (4)$$

where M is the number of delta functions, w_i and x_i are the associated quadrature weights and abscissas (or locations) for each of the delta functions. Note that the quadrature weights and abscissas are time-dependent quantities, which are evolved based on evolution equations for selected statistical moments. These moment evolution equations can be derived from the underlying Fokker–Planck equation. Analogous to the moving or adaptive grid based methods for solution of partial differential equations, it is hypothesized that the adaptive (or time dependent) nature of quadrature weights and abscissas will have similar advantages especially in the context of capturing characteristic behavior (e.g. evolution of moments up to a chosen order) using fewer quadrature nodes and hence leading to improvements in computational efficiency. The latter improvements could be particularly useful in the context of problems where the underlying distributions undergo significant changes (e.g. unimodal PDF to bimodal PDF, and with significantly different mean values) during their evolution under the influence of stochastic dynamics (with or without stochastic feedback). Traditional methodologies for solution of Fokker–Planck equations based on standard or fixed quadrature relying on orthonormal functions may

be inadequate when the fixed basis functions initially chosen become inefficient choices during the course of evolution of the PDF (undergoing significant changes in characteristic behavior). Basis functions that can adapt to the changing dynamics may appear to be more desirable for improvements in computational efficiency and the DQMOM approach offers a class of such basis functions that can adapt according to changes in the PDF over time. As such significant structural changes in the characteristic behavior of systems are commonly found in nonlinear Fokker–Planck equations (e.g. the nonlinear Fokker–Planck equation corresponding to the Desai–Zwanzig model, where the evolution of the PDF exhibits transient bimodality), the application of the direct quadrature method of moments to nonlinear Fokker–Planck equations may be worth exploring. Based on the successful applications of DQMOM for solution of linear Fokker–Planck equations in previous works [42, 44, 48, 45], generalizations of DQMOM for solutions of nonlinear Fokker–Planck equations (i.e. the focus of this paper) could be justified.

The initial values of the weights and abscissas can be assigned based on the initial conditions for the PDF (and hence the moments). From the weights and abscissas, the generalized moments can be determined for equation (4) using the definition of the generalized moment, $\langle x^r \rangle$:

$$\langle x^r \rangle \equiv \int_{-\infty}^{\infty} x^r f(x, t) dx = \sum_{i=1}^M w_i x_i^r, \quad (5)$$

where r is the superscript corresponding to any moment and the second equality in the above equation is obtained using equation (4). Typically in DQMOM this value is a non-negative integer, but for some applications non-negative fractions may be needed for better accuracy. The evolution of the moments can then directly be found by taking the derivative of equation (5) with respect to time as

$$\begin{aligned} \frac{\partial \langle x^r \rangle}{\partial t} &= -x^r D(x, t, f) f(x, t) \Big|_{-\infty}^{\infty} + r \int_{-\infty}^{\infty} x^{r-1} D(x, t, f) f(x, t) dx \\ &+ r(r-1) \int_{-\infty}^{\infty} x^{r-2} Q(x, t, f) f(x, t) dx. \end{aligned} \quad (6)$$

As the first term on the right-hand side is zero (due to boundedness and continuity of moments), the above equation can be expressed as

$$\frac{\partial \langle x^r \rangle}{\partial t} = r \langle x^{r-1} D(x, t, f) \rangle + r(r-1) \langle x^{r-2} Q(x, t, f) \rangle. \quad (7)$$

Using equations (4), (5) and (7) the above equation can be further expressed in terms of the adaptive weights and abscissas, as

$$\sum_{i=1}^M (1-r) x_i^r \dot{w}_i + \sum_{i=1}^M r x_i^{r-1} \dot{\zeta}_i = r \sum_{i=1}^M w_i x_i^{r-1} D(x_i, t, w_i) + r(r-1) \sum_{i=1}^M w_i x_i^{r-2} Q(x_i, t, w_i), \quad (8)$$

where $\zeta(t) \equiv w(t)x(t)$ denotes a weighted abscissa. The above represents a set of equations as $Az = b$ for a selected set of $2M$ constraints on low order moments (obtained for different values of r), needed to solve for M undetermined weights and M undetermined abscissas. Here, the right-hand side of equation (8) constitutes an element of the b vector and

$z = [\dot{w}_1 \cdots \dot{w}_M \dot{\zeta}_1 \cdots \dot{\zeta}_M]^T$ denotes a vector of weights and weighted abscissas. The vector z is obtained as a solution of the system $Az = b$, from which the weights and abscissas can be derived via integration of a system of ordinary differential equations. Note that unlike in the case of linear FPE, the right-hand side of equation (8) can have a nonlinear dependence on weights for general nonlinear Fokker–Planck equations.

The DQMOM formulation is also straightforward for multivariate cases. To formulate DQMOM for a three-dimensional problem, instead of equation (4), the following is used for the weighted summation of Dirac delta functions:

$$f(\mathbf{x}, t) = \sum_{i=1}^M w_i \prod_{k=1}^{N_d} \delta(x_k - x_{k_i}), \quad (9)$$

where N_d is the number of dimensions and it is evaluated at x_i and w_i . Equation (9) is then substituted into equation (3). After this substitution the following definition for generalized mixed moments is used to arrive at the final nonlinear differential equation:

$$\left\langle \prod_{k=1}^{N_d} x_k^{r_k} \right\rangle = \int_{-\infty}^{\infty} \left(\prod_{k=1}^{N_d} x_k^{r_k} \right) f(\mathbf{x}, t) \, d\mathbf{x} = \sum_{i=1}^M w_i \left(\prod_{k=1}^{N_d} x_{k_i}^{r_k} \right). \quad (10)$$

In the following sections, we will illustrate the accuracy of DQMOM for the solution of both linear and nonlinear Fokker–Planck equations.

3. Linear Fokker–Planck equation in one dimension

The first type of Fokker–Planck equation considered is a linear FPE describing the Ornstein–Uhlenbeck (OU) process, which is commonly used to describe the Brownian motion of particles in the presence of a frictional force proportional to velocity [49]. For our case, the probability density function represents the probability that the particle will have a given velocity at a certain time as it moves in the gas. Due to the availability of analytic solutions to the Ornstein–Uhlenbeck FPE, it was chosen to verify the accuracy of DQMOM for simple linear FPEs.

To derive the FPE for the Ornstein–Uhlenbeck process, we first start with the Ito–Langevin form of the OU process given by [2]

$$\frac{dX(t)}{dt} = -\gamma X(t) + \sqrt{Q}\Gamma(t), \quad (11)$$

where the diffusion, Q , is a constant and the drift is given by γ . Using the drift and diffusion coefficients, an equivalent Fokker–Planck equation in one dimension is now written using the probability density function $f(\mathbf{x}, t)$:

$$\frac{\partial f}{\partial t} = \gamma \frac{\partial f x}{\partial x} + Q \frac{\partial^2 f}{\partial x^2}. \quad (12)$$

Analytic and stationary solutions are known for the OU FPE, and the analytic solution of the mean and variance is given as [2]

$$M_1(t, t') = \exp^{-\gamma(t-t')}, \quad (13)$$

$$M_2(t, t') = \frac{Q}{\gamma} [1 - \exp^{-2\gamma(t-t')}]. \quad (14)$$

The Ornstein–Uhlenbeck (OU) process was analyzed in one dimension using four nodes. The basic idea behind choosing the initial values for quadrature weights and abscissas is to ensure that moments up to a selected order (from a chosen selection of moment constraints) evaluated using the initial selection for quadrature weights and abscissas match the corresponding moments of the initial distribution. While the initial quadrature weights and initial abscissas can be related to the initial moments via a set of nonlinear algebraic equations, as $\sum_{i=1}^M w_i(t) x_i^r(t) = \langle x^r \rangle$, for M distinct chosen values of r , the solution of this system can often be cumbersome (especially for large values of M). Hence, more direct approaches that rely only on matching the first few moments (e.g. up to covariance) are sought. The effects of initial error in mismatch of selected high order moments can be assessed by comparisons with other methods.

The initial condition of interest for the OU process is a Dirac delta function located at unity. This Dirac delta function should now be represented in terms of our quadrature weights and abscissas such that the overall system is non-singular. Note that the selection procedure for quadrature weights and abscissas is non-unique and that singularities in DQMOM can arise when the locations of any two of the quadrature nodes become identical and/or if the rows of the A matrix become linearly dependent. Given these restrictions, the initial conditions for the quadrature weights and abscissas are selected such that the following conditions are satisfied: (a) the zeroth moment $\langle x^0 \rangle$ is unity (due to the normalization property for probability density functions), (b) the initial value of the mean $\langle x \rangle = 1$, (c) the initial value of the variance is close to zero and (d) the skewness is zero. This allows us to select the following set of initial values for the weights: $w_1(0) = w_2(0) = w_3(0) = w_4(0) = 0.25$ (among many other possibilities). The abscissas are selected such that $[x_1(0) \ x_2(0) \ x_3(0) \ x_4(0)] = [\mu - b\sigma \ \mu - a\sigma \ \mu + a\sigma \ \mu + b\sigma]$, where μ is the initial mean, σ is the initial standard deviation, which is set to a small value, say 10^{-4} . In order to ensure consistency with the initial choice of weights and variance, we solve for a and b and obtain $a = 0.5^{1/2}$ and $b = 1.5^{1/2}$ (as one of the many possible solutions). The quadrature weights and abscissas are evolved such that the evolution equations for a set of moments are satisfied. The number of moment constraints needed is equal to the number of unknowns, including weights and abscissas (i.e. eight moment equations are needed in order to obtain the evolution of four quadrature weights and four abscissas, in one-dimensional space). We select the following moment constraints or evolution equations for the moments: $\langle x^r \rangle$, for $r = 0-7$. The evolution equation for the moments can be derived from the underlying Fokker–Planck equation for the OU process, as

$$\frac{\partial \langle x^r \rangle}{\partial t} = -\gamma r \langle x^r \rangle + r(r-1)Q \langle x^{r-2} \rangle. \quad (15)$$

The corresponding equations governing the time evolution of quadrature weights and (weighted) abscissas can be inferred from equation (8). These evolution equations for quadrature weights and (weighted) abscissas can be integrated to obtain the new values of quadrature weights and (weighted) abscissas over a small time interval, given their initial conditions. This integration procedure can be iteratively repeated to obtain the quadrature weights and abscissas for all time, which can further enable us to deduce the evolution of moments for all time.

The comparison of DQMOM with the exact transient solution for the mean, M_1 , is illustrated in figure 1(a). The exact solution is represented by the diamonds, and DQMOM

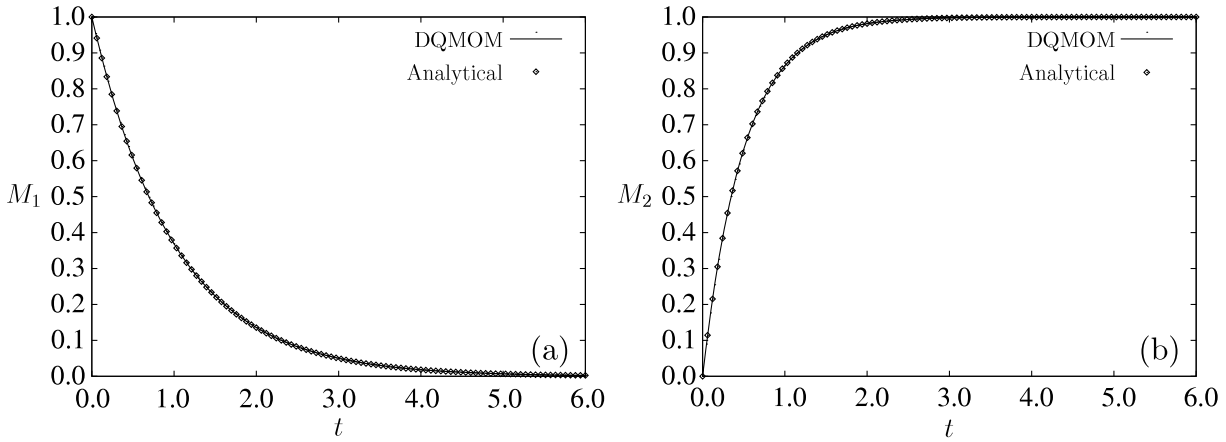


Figure 1. Results of (a) mean, M_1 , and (b) variance, M_2 , with $\gamma = Q = 1$. The DQMOM results (solid lines) using four quadrature nodes agree with the analytic solutions (diamonds).

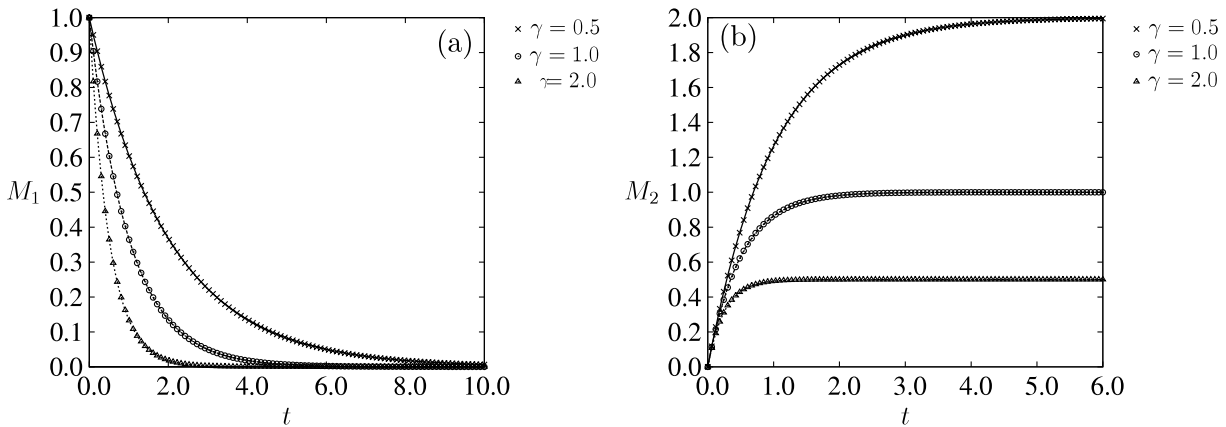


Figure 2. Results of (a) mean, M_1 , and (b) variance, M_2 , for $Q = 1$ and $\gamma = 0.5, 1.0, 2.0$. The DQMOM results using four quadrature nodes for each γ are shown by solid lines ($\gamma = 0.5$), dashed lines ($\gamma = 1.0$) and dotted lines ($\gamma = 2.0$). The corresponding analytical solutions are indicated by cross, circle and triangle symbols respectively.

is represented by the solid line. The mean is physically the average velocity of the free particle in Brownian motion. The results obtained from DQMOM for the variance are plotted against the analytic solution for the variance, $M_2 = \langle x(t)^2 \rangle - \langle x(t) \rangle^2$, in figure 1(b). As shown, the results obtained from DQMOM match the exact solution for the mean and variance.

Due to the friction term, γ , it is expected that the velocity of the particle will decrease to zero as time increases. As the friction increases, it is also expected that the rate of decay to zero velocity should also increase. This qualitative explanation is verified quantitatively by equation (13) and is clearly shown in figure 2(a), presenting the evolution of the mean values of the Ornstein–Uhlenbeck process for three separate drift coefficients, γ , using DQMOM. The evolution of the variance for the same drift values used in figure 2(a) is

shown in figure 2(b). From the stationary solution, the values of the variance should approach the value Q/γ . A larger value of γ not only results in a faster approach to equilibrium, but also in a smaller equilibrium value.

The results in this section show that DQMOM can match exactly the transient solution for a linear Fokker–Planck equation following the Ornstein–Uhlenbeck process. Hence the accuracy of DQMOM for capturing transient solutions of linear Fokker–Planck equations is validated. We will now apply DQMOM to the solution of nonlinear Fokker–Planck equations and the results will be described in section 4.

4. Nonlinear Fokker–Planck equations

This section consists of three subsections. The comparison of results from DQMOM to the analytic stationary and transient solutions of the Shimizu–Yamada model for muscular contraction is presented in section 4.1. Section 4.2 compares the results from DQMOM to those obtained by Drozdov [27] and Zhang *et al* [26] for the Desai–Zwanzig model. The discussion of nonlinear Fokker–Planck equations finishes with section 4.3 which presents results obtained from DQMOM for fermions and bosons, and compares the results to the analytic stationary solution.

4.1. The Shimizu–Yamada model

The Shimizu–Yamada (SY) model [23, 50] was phenomenologically derived as a way to describe muscular contractions from a hydrodynamic perspective. Muscular contractions are caused by mutual sliding of myosin and actin filaments with cross-bridges extending from the myosin to the actin filaments, and the force for the sliding motion is between the terminal part of the cross-bridge and the actin [23, 50, 24, 2]. Shimizu and Yamada [23] considered the cross-bridges to be a subsystem making up the supersystem which is the sliding motion of the filaments. Relating this biological interaction of a subsystem with a supersystem during muscular contraction to a hydrodynamic system, the cross-bridge subsystem is analogous to particles in a fluid, and the filament supersystem is considered to be the macroscopic fluid [23, 50, 24]. The model is then derived for the velocity of certain muscular tissue [23, 50]. As there exist exact stationary and transient solutions to this model, it is desired to compare DQMOM results to this nonlinear Fokker–Planck equation as a benchmark test of DQMOM for a nonlinear system.

The Ito–Langevin equation for the Shimizu–Yamada model is given as [28]

$$\frac{dX(t)}{dt} = -\gamma X(t) - \kappa (X(t) - \langle X(t) \rangle) + \sqrt{Q}\Gamma(t), \quad (16)$$

where γ and κ make up the drift coefficient. From the Langevin equation, it becomes apparent that when $\kappa = 0$, the Shimizu–Yamada model reduces to the linear Ornstein–Uhlenbeck process. Also, from the Langevin equation it is clear that the transient mean will behave in the same way for both the OU process and the Shimizu–Yamada model no matter what the value of κ is. The Shimizu–Yamada model is then, in terms of the probability density function [23, 51],

$$\frac{\partial}{\partial t} f(x, t) = \frac{\partial}{\partial x} [\gamma x + \kappa (x - \langle X \rangle)] f + Q \frac{\partial^2}{\partial x^2} f. \quad (17)$$

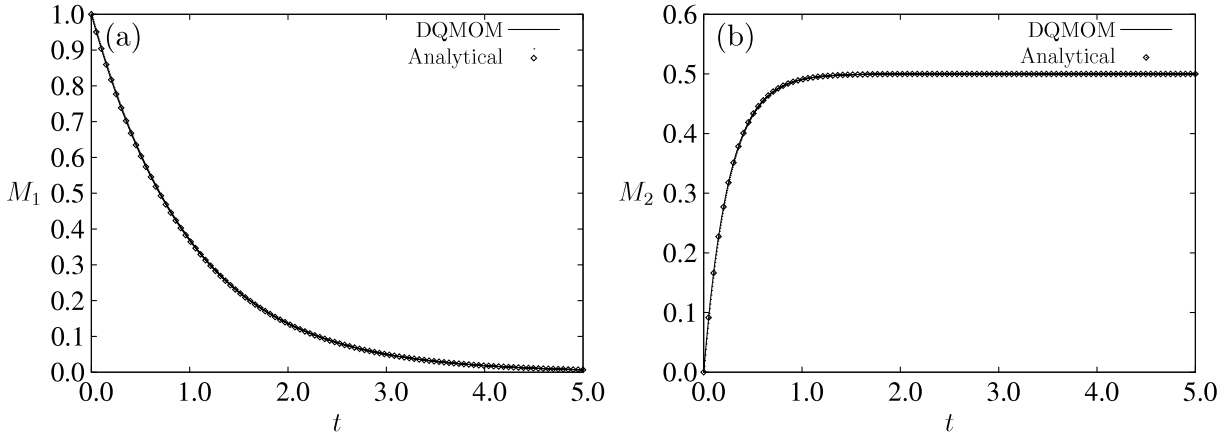


Figure 3. Results of (a) mean, M_1 , and (b) variance, M_2 , with $\gamma = \kappa = Q = 1$ for the Shimizu–Yamada model, equation (17). The solid lines denote results from DQMOM using four nodes and the symbols denote analytical results.

While the transient variance of the SY model is not the same as that of the OU process, it is similar, the only difference being the addition of κ with γ , instead of just γ in the denominator and in the exponential. The equations for the transient mean and variance are given in equations (18) and (19) respectively [51]:

$$M_1(t, t') = \exp^{-\gamma(t-t')}, \quad (18)$$

$$M_2(t, t') = \frac{Q}{\gamma + \kappa} [1 - \exp^{-2(\gamma+\kappa)(t-t')}] . \quad (19)$$

To validate the accuracy of DQMOM in representing the solution of the nonlinear Fokker–Planck equation corresponding to the Shimizu–Yamada model, we consider four quadrature nodes as before, with the same set of initial conditions on quadrature weights and abscissas as selected for the OU processes. The moment constraints are also set to be identical to those described earlier for the OU process. Computational results obtained from DQMOM (solid line) compared with the analytical results given by equations (18) and (19) are shown in figure 3. In one dimension, the coefficients γ , κ and Q were all one and DQMOM used four quadrature nodes. As shown by figure 3(a) the DQMOM result for the transient mean is in excellent agreement with the analytic solution for the transient mean. Excellent agreement between DQMOM and the exact analytical solution for the transient variance is also shown in figure 3(b). Now that the accuracy of DQMOM for a simple nonlinear Fokker–Planck equation has been shown, it is desired to show that DQMOM can also be used to obtain accurate results for complex nonlinear FPEs.

4.2. The Desai–Zwanzig model

The Desai–Zwanzig (DZ) model gives a more general description than the SY model for muscular contractions and can be thought of as the velocity of multiple connected oscillators [25, 2]. The idea that the DZ model describes multiple oscillators allows for many applications, including a three-dimensional case where this model can describe

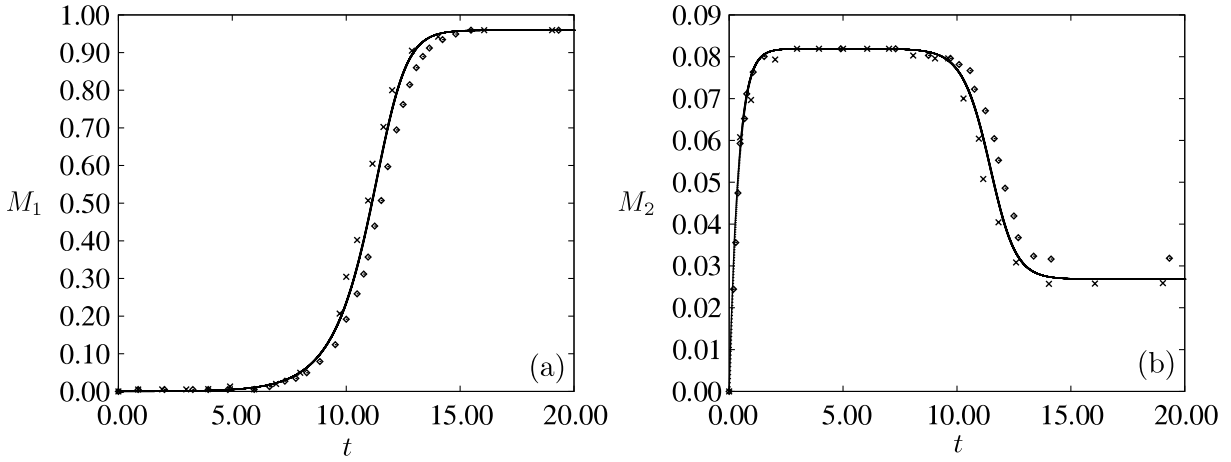


Figure 4. Results of (a) mean, M_1 , and (b) variance, M_2 , with $\gamma = b = 1$, $\kappa = 2.0$, and $Q = 0.1$ for the Desai–Zwanzig model, equation (22). The solid line is from DQMOM, the diamonds are from Drozdov and Morillo [27], and the the crosses are from Zwanzig and Desai [25].

oscillators arranged in a lattice. For this case, the oscillators represent the atomic forces on atoms arranged in the lattice. The Ito–Langevin equation derived in [28] for the Desai–Zwanzig model is

$$\frac{dX(t)}{dt} = U'(X, t) + \sqrt{Q}\Gamma(t), \tag{20}$$

where U' is the differential of the kinetic potential with respect to x , and is then given as

$$U'(X, t) = \gamma X(t) - bX(t)^3 - \kappa(X(t) - \langle X \rangle). \tag{21}$$

From the above equations, the FPE for the DZ model in terms of the probability density function is given as

$$\frac{\partial}{\partial t} f(x, t) = -\frac{\partial}{\partial x} [\gamma x - bx^3 - \kappa(x - \langle X \rangle)] f + Q \frac{\partial^2}{\partial x^2} f. \tag{22}$$

The DZ model has the property that when $\kappa = 0$ it becomes a linear FPE and when $b = 0$ it reduces to the Shimizu–Yamada model. Another property of the Desai–Zwanzig model is that it displays strong bimodality. This was researched extensively by Drozdov and Morillo [27] and Zhang *et al* [26] and their results are compared with those obtained from DQMOM. It was unknown how well DQMOM could capture this bimodality, which is one reason for the Desai–Zwanzig model being chosen to study. Another reason for choosing this model is the large number of applications it has, so an efficient method to solve the DZ model is desired.

While the DZ model does possess transient bimodality, it does not appear until the diffusion coefficient is small compared to the drift coefficient. An example of this is clearly seen in figure 4 where $Q = 0.1$ and $\kappa = 2.0$. Figure 4(a) shows the comparison of the mean computed by DQMOM, represented by a solid line, to a sixth-order cumulant moments method [25] and a finite-differencing scheme [25, 27], represented by crosses and diamonds, respectively. Zwanzig and Desai obtained their results using a sixth-order

J. Stat. Mech. (2011) P09031

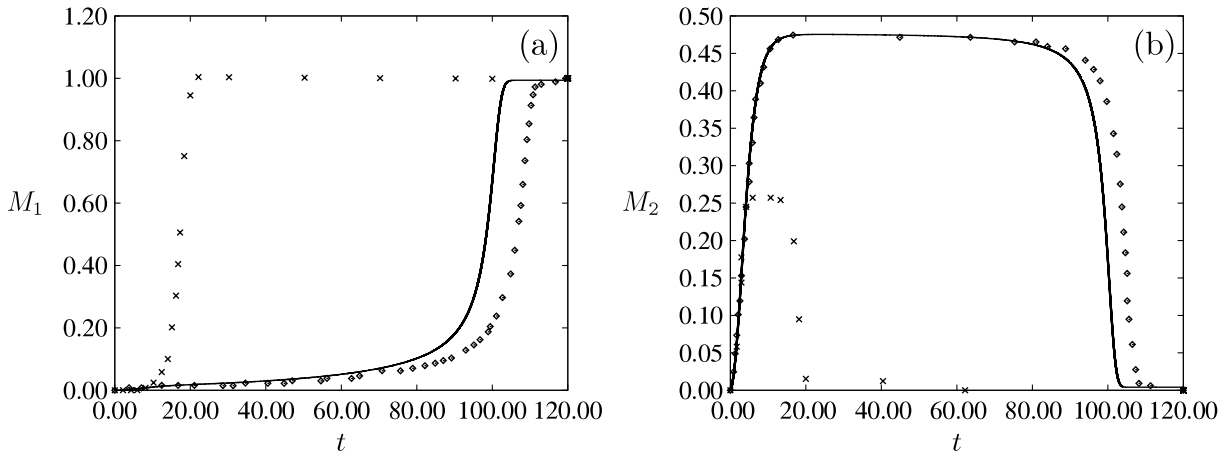


Figure 5. Results of (a) mean, M_1 , and (b) variance, M_2 , with $\gamma = b = 1.0$, $\kappa = 0.5$, and $Q = 0.01$. In each subfigure, DQMOM (solid line), cumulant moment method [27] (crosses), and DAF [26] (diamonds) results are compared.

cumulant moment method which has the fastest convergence time out of the three, and reaches the same stationary solution for the mean as the other two methods. The finite-differencing scheme developed by Drozdov and Morillo [27] to analyze the Desai–Zwanzig model has the slowest convergence time. DQMOM is shown to be just as accurate for the stationary solution, and is close to the other methods during the transient behavior.

The variance of the Desai–Zwanzig model is illustrated in figure 4(b) using the same values for the drift and diffusion as in figure 4(a). All three of the methods obtain the same maximum transient variance value, but spend different times at that value. The cumulant moment method appears to have the fastest convergence time, leaving the maximum the soonest and converging to the lowest stationary variance. The finite-differencing scheme stays the longest at the maximum, and reaches the largest stationary mean value. All three of these methods follow the same trend with DQMOM following the cumulant moment method more closely, but the results of DQMOM fall in between the results from the other two methods.

As shown in figures 4(a) and (b), our moment method (i.e. DQMOM) works well for monostable systems. As the DZ model exhibits bistability under certain conditions, it would be interesting to investigate whether DQMOM can indeed capture such behavior. It is shown in figure 5, where $\kappa = 0.5$ and $Q = 0.01$, that DQMOM is indeed able to capture this bistability. The evolutions of mean and variance are shown in figures 5(a) and (b) respectively, where the results obtained from DQMOM are compared with those obtained by Desai and Zwanzig [25] and Zhang *et al* [26]. Zhang *et al* [26] obtained their results by applying a distributed approximating functional (DAF) based method using a polynomial of degree 54 to approximate the Dirac delta function, $\delta(x-x')$. Note that the predictions of transient behavior for mean, M_1 , and variance, M_2 , obtained from the cumulant moment method are qualitatively different (and inaccurate) compared to DAF and DQMOM. This discrepancy is due to known limitations [26, 27] of the cumulant moment method in capturing transient bimodality, although the cumulant moment method works well for systems that remain monostable for all time [26, 27]. For bistable systems, the cumulant

moment hierarchy is known to converge very slowly. While the saturation plateau values and saturation time scales for M_2 obtained from DAF and DQMOM are in reasonable agreement, the corresponding values obtained from the cumulant moment method are different (the saturation time scales for M_1 are observed to be much shorter and the transient plateau value for M_2 is much smaller for the cumulant moment method).

Note that the comparison shown in figure 5 only required that 15 quadrature nodes were used in DQMOM. This is equivalent to 30 variables (including 15 quadrature weights and 15 abscissas/locations of the delta functions) in DQMOM (to be compared with the computational cost of using a 54 degree polynomial to approximate the delta function in DAF). In addition to the number of quadrature nodes to be specified in DQMOM to achieve these results, the initial mean and variance also had to be set. The initial mean value was given by Zhang *et al* [26] as $x_0 = 10^{-4}$, but the initial variance was not given. Knowing that DAF approximates a Dirac delta function, the initial variance can be set for DQMOM. For this simulation a value of 10^{-11} for the initial variance was used. It was observed, however, that as the initial variance was increased, the transient bimodality existed for longer. This is most likely due to the sensitivity of the system to initial conditions.

To analyze the characteristics of the bimodality further, the probability density function (PDF) at various time steps was computed from the moments using a maximum entropy method [52], subject to moment constraints. In our approach the moments are obtained via DQMOM and the entropy is maximized subject to the chosen moment constraints. The kinetic and effective potentials [26] are shown for reference in figures 6(a)–(d) to show some characteristic features of the Desai–Zwanzig model which has an unusual bimodality in that there is no ‘flat’ region in the kinetic potential. Drozdov and Morillo [27] were among the first to observe this behavior, which was confirmed by Zhang *et al* [26]. The case of $\kappa = 0.5$ and $Q = 0.01$ was analyzed for comparison and is shown in figures 6(a)–(d), where the diamonds represent the results from Zhang *et al* [26], and the solid line those from DQMOM. The dotted line is the kinetic potential, and the dashed line is the effective potential, $V(x, t)$, given below:

$$V(x, t) = \frac{[x^3 + x - \kappa(x - \langle X(t) \rangle)]^2}{4Q} - \frac{1}{2}(3x^2 + \kappa - 1). \quad (23)$$

The PDFs show good agreement at $t = 1$ s (figure 6(a)), and $t = 72$ s (figure 6(c)) while for $t = 4$ s (figure 6(b)) the PDFs differ slightly. At the time $t = 105.5$ s (figure 6(d)), however, the PDFs differ greatly. DQMOM has already reached an equilibrium value at $t = 105.5$ s, while the method of Zhang *et al* [26] has not yet reached the equilibrium value, but is close.

Even though the bistability should last longer as the diffusion decreases compared to the drift term, for very small values of the diffusion this is not the case. This is captured by DQMOM, Monte Carlo and by the DAF method used by Zhang *et al* [26]. According to Zhang *et al* [26] this is due to the nonlinearity of the system being much larger for this case than for the other cases. This large nonlinearity dominates the physical process, only allowing a very short-lived bimodality. For DQMOM to capture this and obtain a similar transient solution to Zhang *et al* [26] the number of quadrature nodes was again 15, and the initial variance value was 10^{-11} . The DZ model for the mean and variance shown in figure 7 uses $\gamma = 1.0$, $\kappa = 0.5$, and $Q = 0.0001$. Monte Carlo is introduced to show

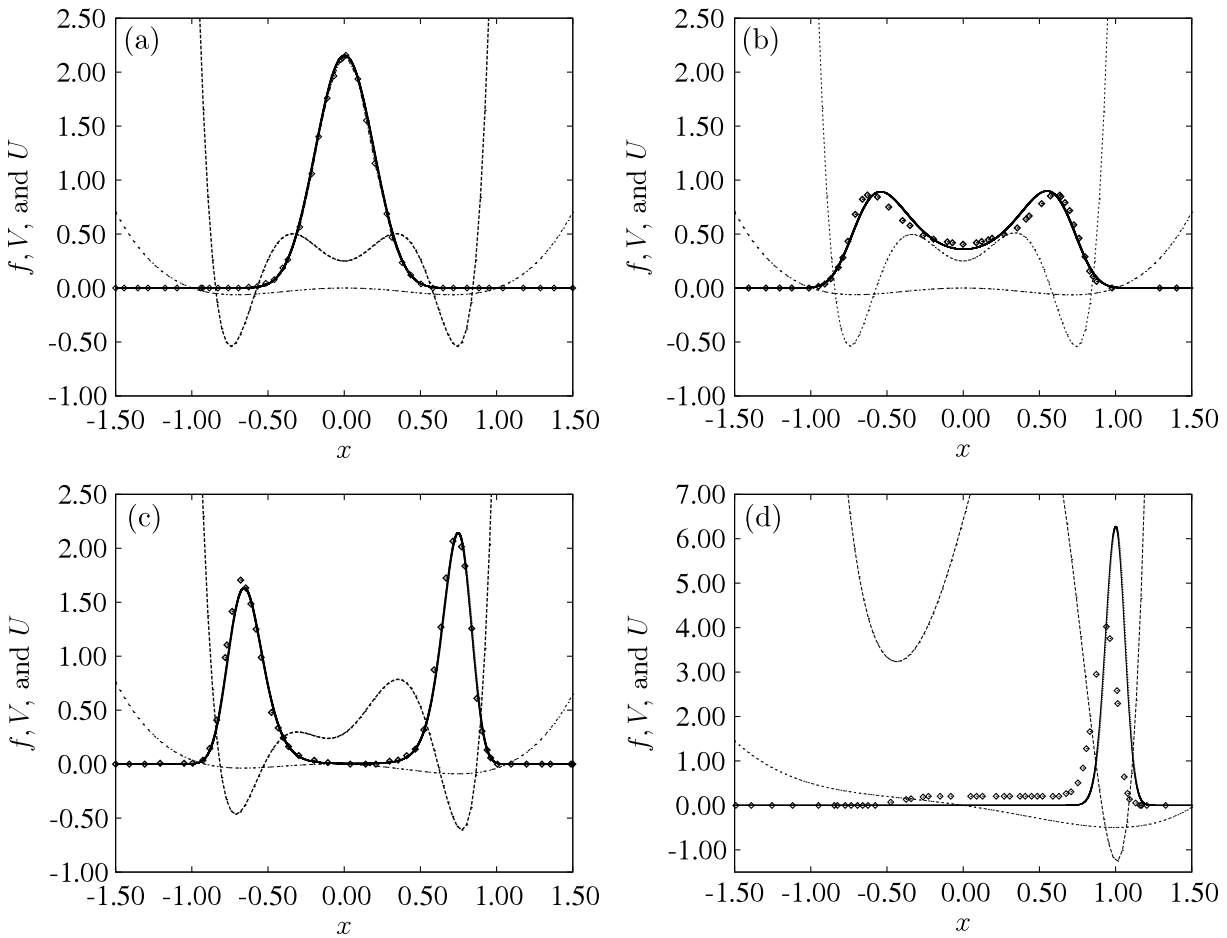


Figure 6. The plots show the PDF, f (solid line), the effective potential, V (dashed line), and the kinetic potential (dotted line) from DQMOM. Results for the PDF from Zhang *et al* [26] are shown by diamonds with $\gamma = b = 1.0$, $\kappa = 0.5$, $Q = 0.01$, and $\langle x(0) \rangle = 10^{-4}$. (a) $t = 1.0$ s, (b) $t = 4.0$ s, (c) $t = 72$ s, and (d) $t = 105.5$ s.

the efficiency of DQMOM in obtaining a solution. This Monte Carlo code was written to solve the equivalent Langevin equation for the Desai–Zwanzig model and uses one million samples. Using one processor, DQMOM was able to obtain a solution in approximately 3 min of computational time. For the same values of γ , κ and Q , it took Monte Carlo 18 min of computational time using 32 processors and one million samples. Due to the sensitivity of the system to initial conditions, the methods do not exactly match during their evolution. However, their evolutions are close, and have the same stationary values. Also, since the diffusion term is small, this case is more computationally intensive to maintain sufficient accuracy.

While the Desai–Zwanzig model was more complex than the Shimizu–Yamada model, they are both equations which describe muscular contractions. A nonlinear Fokker–Planck equation for a different application is desired to show the versatility of DQMOM. The next equation studied is a Fokker–Planck equation for particles which follow Fermi–Dirac statistics.

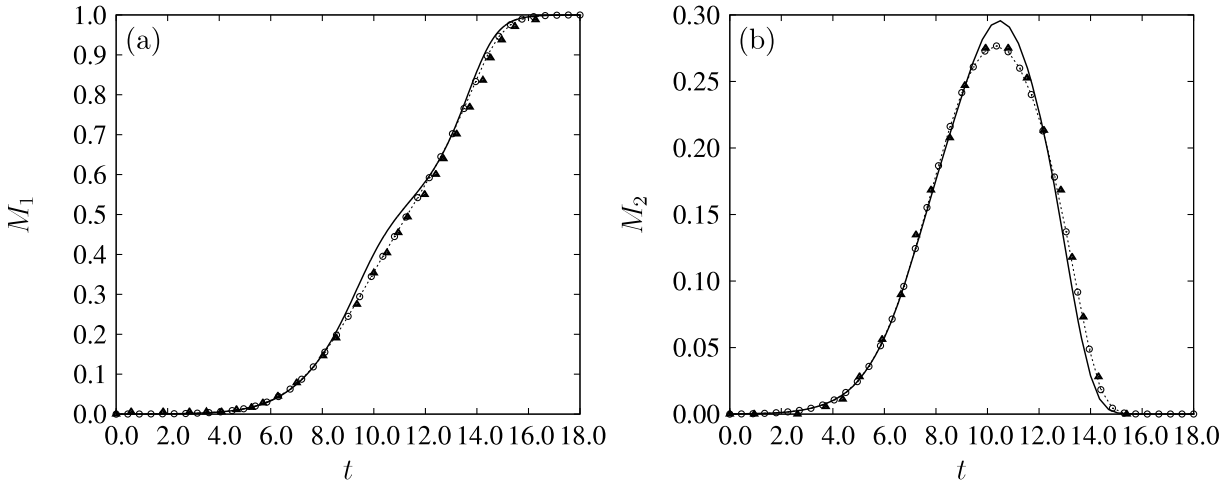


Figure 7. Results of (a) mean, M_1 , and (b) variance, M_2 , for the Desai–Zwanzig model with $\gamma = b = 1.0$, $\kappa = 0.5$, and $Q = 0.0001$ corresponding to DQMOM (lines), the Monte Carlo method (circles), and DAF [26] (triangles).

4.3. Fermions and bosons

Fermions or particles following Fermi–Dirac statistics (FD) obey the Pauli exclusion principle (EP) which states that for systems composed of either elementary material particles or atoms and molecules composed of an odd number of them, no quantum energy state may contain more than one particle. In contrast, particles that obey Bose–Einstein (BE) statistics or bosons are not constrained by the exclusion principle and a large number of particles can occupy the same quantum state. The behavior of particles obeying a generalized exclusion–inclusion Pauli principle (EIP) has also been studied by Kaniadakis and Quarati [6, 7] via the introduction of (a) a continuous parameter κ ranging from -1 to 1 to represent the degree of indistinguishability (or classicality) of the particles and (b) enhancement or inhibition factors based on occupation numbers. These authors also derived the corresponding nonlinear Fokker–Planck equations (based on enhancement and inhibition factors) and the underlying stationary distributions, which give FD statistics for $\kappa = -1$, BE statistics for $\kappa = +1$, Maxwell–Boltzmann statistics for $\kappa = 0$ and intermediate statistics for all other values. In this section, we are interested in exploring the transient and stationary solutions of the Fokker–Planck equations for fermions using DQMOM. The FPE for particles obeying Fermi–Dirac statistics and Bose–Einstein statistics obtained from [6, 7] is given below, where the upper sign corresponds to the BE and the lower sign corresponds to the FD case:

$$\frac{\partial}{\partial t}n(t, v) = -\frac{\partial}{\partial v}k_1(v)[1 \pm n(t, v)]n(t, v) + k_2\frac{\partial^2}{\partial v^2}n(t, v), \quad (24)$$

where

$$k_1 = cv, \quad k_2 = \frac{c}{\beta m}, \quad \beta = \frac{1}{kT} \quad (25)$$

and k is the Boltzmann constant, T is the absolute temperature and m is the mass. Note that a similar nonlinear Fokker–Planck equation can also be derived using momentum space instead of velocity space.

Taking the flux of the particles into account and making the energy a variable, from equation (24) Kaniadakis [7] derived the following equation:

$$\frac{\partial n(t, E)}{\partial t} = \frac{2c}{E^{1/2}} \frac{\partial}{\partial E} \left(E^{3/2} \left\{ n[1 \pm n] + \frac{1}{\beta} \frac{\partial n}{\partial E} \right\} \right). \quad (26)$$

Introducing the occupational probability, $p(t, E)$, into equation (26) gives the following Fokker–Planck equation which is solved using DQMOM:

$$\frac{\partial p}{\partial t} = -2c \frac{\partial}{\partial E} \left[- \left(E + \frac{1}{2\beta} \pm \frac{\sqrt{E}}{\theta} p \right) p \right] + \frac{2c}{\beta} E \frac{\partial^2 p}{\partial E^2}, \quad (27)$$

where $\theta = 2\pi(2/m)^{3/2}$ and comes from the fact that the particles are spherical. The derivation for this is found in the appendix.

The stationary solution for equation (27) is given by

$$p_{\text{st}}(E) = \frac{\theta E^{1/2}}{\exp\{[E - \mu]/kT\} \mp 1}, \quad (28)$$

where μ is the integration constant. When the temperature is less than the Fermi temperature, μ can be approximated as the Fermi energy.

To compare the results for DQMOM to the analytic stationary moment results obtained from equation (28), the integration constant had to be determined numerically using MapleTM. Once μ was determined, the moments of equation (28) were taken and the results compared to DQMOM. Transient and stationary moment results obtained from DQMOM (for $kT = 1$ and $\theta = 1$) are compared to the analytic stationary moment results in figure 8. To increase the accuracy of DQMOM, a total of nine nodes were required. Unlike the previous applications of DQMOM where non-negative integer moment constraints were used, this application required constraints on the fractional moments as well. Constraints on the evolution of (raw) fractional moments, $\langle E^r \rangle$, for r ranging from 0 to 4.25, in increments of 0.25 were used in DQMOM.

5. Conclusion

In this work, we present (for the first time) the development and application of an efficient and accurate computational method, the direct quadrature method of moments (DQMOM) for the solution of nonlinear Fokker–Planck equations. DQMOM features the representation of a probability density function using a finite collection of Dirac delta functions characterized by unknown quadrature weights and abscissas. The weights and abscissas are adaptive in time and are obtained from constraints on the evolution of generalized moments. It may be noted that in the case of a one-dimensional nonlinear Fokker–Planck equation (where the drift and diffusion coefficients can be functions of the underlying probability density function), a DQMOM based numerical solution using M nodes (where each node i is characterized by a weight $w_i(t)$ and abscissa location $x_i(t)$) involves solution of $2M$ evolution equations for moments (e.g. $\{M_0, M_1, \dots, M_{2M-1}\}$) from which the evolution of (M) weights and (M) abscissa locations can be determined (for all time). The time adaptive feature of these quadrature nodes (in contrast to fixed node quadrature) is particularly useful in improving the computational efficiency, especially

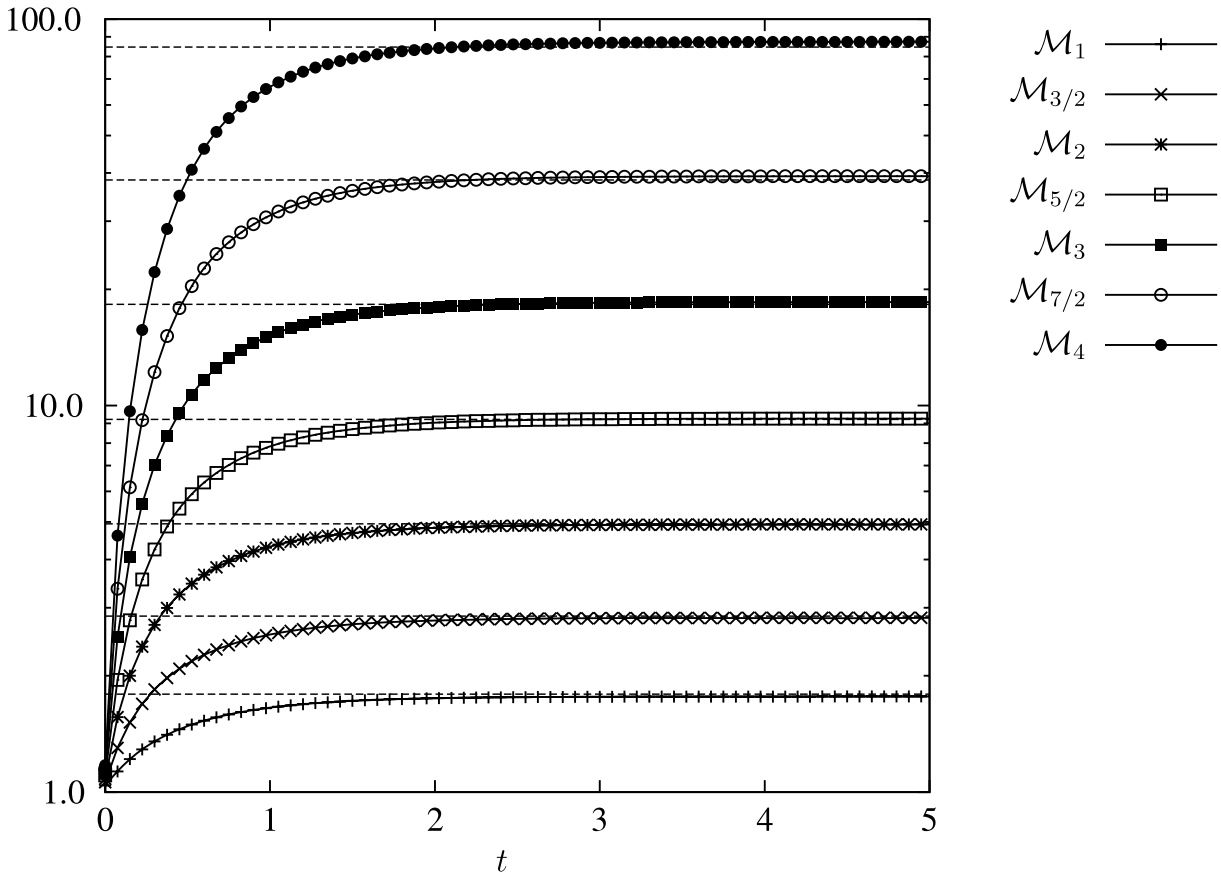


Figure 8. Transient and stationary behavior of (selected integer and fractional) raw moments obtained from equation (27), which describes the distribution of particles obeying Fermi–Dirac statistics. The dashed lines represent exact stationary solutions obtained from a stationary Fermi–Dirac distribution. For the cases shown here, $kT = 1.0$ and $\theta = 1.0$.

in the context of problems where the underlying distributions undergo significant changes during their evolution under the influence of stochastic dynamics (with or without stochastic feedback). Generalization of the DQMOM formulation for solution of multivariate nonlinear Fokker–Planck equations is also developed in this paper (in section 2). Although DQMOM involves the evolution of moments, it is shown that important features of the probability density functions (e.g. multimodal probability distributions) can be reconstructed accurately based on the moments using the maximum entropy method.

Using no more than four quadrature nodes, DQMOM was applied to the linear Fokker–Planck equation describing the Ornstein–Uhlenbeck process. Then DQMOM was applied to the nonlinear Fokker–Planck equations describing the Shimizu–Yamada model, the Desai–Zwanzig model, and particles which obey Fermi–Dirac and Bose–Einstein statistics. Where available, the results have been compared with analytic transient and stationary solutions of the mean and variance, which showed excellent agreement. For the Desai–Zwanzig model, DQMOM was also able to capture the long-lived transient

bimodality, which a cumulant moment method was unable to capture. This bimodality was captured by both a finite-differencing scheme, which is more computationally intensive, and a DAF method using a polynomial approximation of Dirac delta functions of degree 54 [26]. In addition to capturing the long-lived bimodality, DQMOM was also able to efficiently capture a numerical solution of the Desai–Zwanzig model when the diffusion coefficient was small relative to the drift coefficient. This efficiency is most apparent when compared to the computational time and resources required by Monte Carlo. For the solution of most of these FPEs, four quadrature nodes were all that was required. When capturing the bimodality present in the DZ model 15 nodes were required, and nine were required for capturing the transient solution of the Fermi–Dirac FPE. The solution of the Fermi–Dirac FPE also required constraints on the fractional moments, which have been used for the first time in DQMOM.

It was shown in this work that DQMOM can be used to efficiently solve nonlinear Fokker–Planck equations, appearing in a wide range of disciplines. Areas where DQMOM may be beneficial include: plasma Fokker–Planck equations, radiation Fokker–Planck equations, quantum Fokker–Planck equations, and others. In future work DQMOM will be applied to the Fokker–Planck equation for particles following Bose–Einstein statistics, transport phenomena in plasmas, the nonlinear Schrödinger equation and radiation hydrodynamics.

Appendix. Derivation of the Fokker–Planck equation governing fermions and bosons

The appendix shows the derivation of the Fokker–Planck equation for the Fermi–Dirac statistics used by DQMOM from the equation derived by Kaniadakis [7].

Starting with equation (26), we have

$$\frac{\partial n(t, E)}{\partial t} = \frac{2c}{E^{1/2}} \frac{\partial}{\partial E} \left(E^{3/2} \left\{ n[1 \pm n] + \frac{1}{\beta} \frac{\partial n}{\partial E} \right\} \right), \quad (\text{A.1})$$

and using the equation for the occupational probability, p ,

$$p(t, E) = 2\pi \left(\frac{2}{m} \right)^{3/2} \sqrt{E} n(t, E), \quad (\text{A.2})$$

the energy Fokker–Planck equation for the occupational probability density can now be derived.

We define θ as

$$\theta \equiv 2\pi \left(\frac{2}{m} \right)^{3/2}. \quad (\text{A.3})$$

Solving equation (A.2) for n , and substituting that into equation (A.1) yields

$$\frac{\partial}{\partial t} \left(\frac{p}{\theta \sqrt{E}} \right) = \frac{2c}{E^{1/2}} \frac{\partial}{\partial E} \left[E^{3/2} \frac{p}{\theta \sqrt{E}} \left(1 \pm \frac{p}{\theta \sqrt{E}} \right) + \frac{E^{3/2}}{\beta} \frac{\partial}{\partial E} \left(\frac{p}{\theta \sqrt{E}} \right) \right]. \quad (\text{A.4})$$

Expanding equation (A.4) gives

$$\frac{\partial}{\partial t} \left(\frac{p}{\theta\sqrt{E}} \right) = \frac{2c}{E^{1/2}} \frac{\partial}{\partial E} \left[\frac{Ep}{\theta} \pm \frac{E^{1/2}p^2}{\theta^2} + \frac{E^{3/2}}{\beta} \frac{1}{\theta\sqrt{E}} \frac{\partial p}{\partial E} - \frac{1}{2} \frac{1}{\beta} \frac{p}{\theta} \right]. \quad (\text{A.5})$$

Multiplying both sides by $\theta\sqrt{E}$ and expanding the partial derivative yields

$$\frac{\partial p}{\partial t} = 2c \frac{\partial}{\partial E} \left[Ep - \frac{1}{2\beta} p \pm \frac{\sqrt{E}}{\theta} p^2 \right] + \frac{2c}{\beta} \frac{\partial p}{\partial E} + \frac{2c}{\beta} E \frac{\partial^2 p}{\partial E^2}. \quad (\text{A.6})$$

Further simplification of equation (A.6) gives equation (27), as

$$\frac{\partial p}{\partial t} = -2c \frac{\partial}{\partial E} \left[- \left(E + \frac{1}{2\beta} \pm \frac{\sqrt{E}}{\theta} p \right) p \right] + \frac{2c}{\beta} E \frac{\partial^2 p}{\partial E^2}. \quad (\text{A.7})$$

References

- [1] Risken H, 1989 *The Fokker–Planck Equation* (New York: Springer)
- [2] Frank T D, 2005 *Nonlinear Fokker–Planck Equations* (New York: Springer)
- [3] Nicholson D R, 1983 *Introduction to Plasma Theory* (New York: Wiley)
- [4] Takai M, Akiyama H and Takeda S, *Stabilization of drift-cyclotron loss-cone instability of plasmas by high frequency field*, 1981 *J. Phys. Soc. Japan* **50** 1716
- [5] Soler M, Martinez F C and Donoso J M, *Integral kinetic method for one dimension: the spherical case*, 1992 *J. Stat. Phys.* **69** 813
- [6] Kaniadakis G and Quarati P, *Kinetic equation for classical particles obeying an exclusion principle*, 1993 *Phys. Rev. E* **48** 4263
- [7] Kaniadakis G and Quarati P, *Classical model of bosons and fermions*, 1994 *Phys. Rev. E* **49** 5103
- [8] Kaniadakis G, Lavagno A and Quarati P, *Kinetic approach to fractional exclusion statistics*, 1996 *Nucl. Phys. B* **466** 527
- [9] Kaniadakis G, *H-theorem and generalized entropies within the framework of nonlinear kinetics*, 2001 *Phys. Lett. A* **288** 289
- [10] Frank T D and Daffertshofer A, *Nonlinear Fokker–Planck equations whose stationary solutions make entropy-like functionals stationary*, 1999 *Physica A* **272** 497
- [11] Frank T D and Daffertshofer A, *H-theorem for nonlinear Fokker–Planck equations related to generalized thermostatics*, 2001 *Physica A* **295** 455
- [12] Frank T D and Daffertshofer A, *Multivariate nonlinear Fokker–Planck equations and generalized thermostatics*, 2001 *Physica A* **292** 392
- [13] Lapenta G, Kaniadakis G and Quarati P, *Stochastic evolution of systems of particles obeying an exclusion principle*, 1996 *Physica A* **225** 323
- [14] Neumann L and Sparber C, *Stability of steady states in kinetic Fokker–Planck equations for bosons and fermions*, 2008 *Commun. Math. Sci.* **5** 767
- [15] Marsili M and Bray A J, *Soluble infinite-range model of kinetic roughening*, 1996 *Phys. Rev. E* **62** 6015
- [16] Giada L and Marsili M, *First-order phase transition in a nonequilibrium growth process*, 1996 *Phys. Rev. Lett.* **76** 2750
- [17] Barenblatt G I, Entov V M and Ryzhik V M, 1990 *Theory of Fluid Flows Through Natural Rocks* (Dordrecht: Kluwer Academic)
- [18] Crank J, 1975 *The Mathematics of Diffusion* (Oxford: Clarendon)
- [19] Logan J D, 2001 *Transport Modeling in Hydrogeochemical Systems* (Berlin: Springer)
- [20] Sompolinsky H, Golomb D and Kleinfeld D, *Cooperative dynamics in visual processing*, 1991 *Phys. Rev. A* **43** 6990
- [21] Tass P A, *Effective desynchronization with bipolar double-pulse stimulation*, 2002 *Phys. Rev. E* **66** 036226
- [22] Yamana M, Shiino M and Yoshioka M, *Oscillator neural network model with distributed native frequencies*, 1999 *J. Phys. A: Math. Gen.* **32** 3525
- [23] Shimizu H and Yamada T, *Phenomenological equations of motion of muscular contraction*, 1972 *Prog. Theor. Phys.* **47** 350

- [24] Kometani K and Shimizu H, *A study of self-organizing processes of nonlinear stochastic variables*, 1975 *J. Stat. Phys.* **13** 473
- [25] Desai R C and Zwanzig R, *Statistical mechanics of a nonlinear stochastic model*, 1978 *J. Stat. Phys.* **19** 1
- [26] Zhang D S, Wei G W, Kouri D J and Hoffman D K, *Numerical method for the nonlinear Fokker–Planck equation*, 1997 *Phys. Rev. E* **56** 1197
- [27] Drozdov A N and Morillo M, *Solution of nonlinear Fokker–Planck equations*, 1996 *Phys. Rev. E* **54** 931
- [28] Frank T D, *A Langevin approach for the microscopic dynamics of nonlinear Fokker–Planck equations*, 2001 *Physica A* **301** 52
- [29] Ermak D L and Buckholz H, *Numerical integration of the Langevin equation: Monte Carlo simulation*, 1980 *J. Comput. Phys.* **35** 169
- [30] Brey J J, Casado J M and Morillo M, *On the dynamics of a stochastic nonlinear mean-field model*, 1984 *Physica A* **128** 497
- [31] Wehner M H and Wolfer W G, *Numerical evaluation of path-integral solutions to Fokker–Planck equations. III. Time and functionally dependent coefficients*, 1987 *Phys. Rev. A* **35** 1795
- [32] Haken H, *Generalized Onsager–Machlup function and classes of path integral solutions of the Fokker–Planck equation and the master equation*, 1976 *Z. Phys. B* **24** 321
- [33] van Kampen N G, *A soluble model for diffusion in a bistable potential*, 1977 *J. Stat. Phys.* **17** 71
- [34] Tomita H, Ito A and Kidachi H, *Eigenvalue problem of metastability in macrosystem*, 1976 *Prog. Theor. Phys.* **56** 786
- [35] Lax P D, *Nonlinear hyperbolic equations*, 1953 *Pure Appl. Math.* **6** 231
- [36] Forsythe G E and Wasow W R, 1967 *Finite Difference Methods for Partial Differential Equations* (New York: Wiley)
- [37] Palleschi V, Sarri F, Marozzi G and Torquati M R, *Numerical solution of the Fokker–Planck equation: a fast and accurate algorithm*, 1990 *Phys. Lett. A* **146** 378
- [38] Hoffman D K, Nayar N, Kouri D J and Sharafeddin O A, *Analytic banded approximation for the discretized free propagator*, 1991 *J. Phys. Chem.* **95** 8299
- [39] Hoffman D K and Kouri D J, *Distributed approximating function theory: a general, fully quantal approach to wave propagation*, 1992 *J. Phys. Chem.* **96** 1179
- [40] Fox R, 2003 *Computational Models for Turbulent Reacting Flows* (Cambridge: Cambridge University Press)
- [41] Fan R, Marchisio D L and Fox R O, *Application of the direct quadrature method of moments to polydisperse gas–solid fluidized beds*, 2004 *Powder Technol.* **139** 7
- [42] Marchisio D L and Fox R O, *Solution of population balance equations using the direct quadrature method of moments*, 2005 *J. Aerosol Sci.* **36** 43
- [43] Vedula P and Fox R O, *A quadrature-based method of moments for solution of the collisional Boltzmann equation*, *J. Stat. Phys.* under revision
- [44] Attar P J and Vedula P, *Direct quadrature method of moments solution of the Fokker–Planck equation*, 2008 *J. Sound Vib.* **317** 265
- [45] Attar P J and Vedula P, *Direct quadrature method of moments solution of the Fokker–Planck equations in aeroelasticity*, 2009 *AIAA J.* **47** 1219
- [46] Fox R O and Vedula P, *Quadrature-based moment model for moderately dense polydisperse gas-particle flows*, 2010 *Ind. Eng. Chem. Res.* **49** 5174
- [47] Passalacqua A, Vedula P and Fox R O, *Quadrature-based moment methods for polydisperse gas–solid flows*, 2009 *Computational Gas–Solids Flows and Reacting Systems: Theory, Methods and Practice* ed S Pannala, M Syamlal and T O’Brien (Hershey: IGI Global)
- [48] Xu Y and Vedula P, *A quadrature-based method for nonlinear filtering*, 2009 *Automatica* **45** 1291
- [49] Uhlenbeck G and Ornstein L, *On the theory of brownian motion*, 1930 *Phys. Rev.* **36** 823
- [50] Shimizu H, *Muscular contraction mechanism as a hard mode instability*, 1974 *Prog. Theor. Phys.* **52** 329
- [51] Frank T D, *Stochastic feedback, nonlinear families of markov processes, and nonlinear Fokker–Planck equations*, 2004 *Physica A* **331** 391
- [52] Wu N, 1997 *The Maximum Entropy Method* (New York: Springer)